Fermi National Accelerator Laboratory

FERMILAB-Conf-90/159-E
[E-741/CDF]

QCD Studies at the Hadron Colliders *

The CDF Collaboration

presented by

Brenna L. Flaugher
Fermi National Accelerator Laboratory
P.O. Box 500
Batavia, Illinois 60510

August 10, 1990

* Presented at the Xth International Conference on Physics in Collision, Durham, North Carolina, June 21-23, 1990.

Operated by Universities Research Association Inc. under contract with the United States Department of Energy

CDF/PUB/JET/PUBLIC/1274
FERMILAB-CONF-90/159-E
August 10, 1990

QCD Studies at the Hadron Colliders

Brenna L. Flaugher*

Fermi National Accelerator Laboratory

Batavia, Illinois 60510

Abstract

Two hadron collider experiments are actively pursuing QCD jet analyses. They are CDF, with a $\sqrt{s} = 1800$ GeV, and UA2, with a $\sqrt{s} = 630$ GeV. Recent results from these collaborations are discussed. The inclusive jet spectrum, dijet mass and angular distribution are compared to QCD predictions and used to set limits on quark substructure. Data from both experiments are compared to the $O(\alpha_s^3)$ calculations for the inclusive jet cross section. Studies of 3-jet, 4-jet and 5-jet events are described. A limit is set on the cross section for double parton scattering from the UA2 4-jet analysis. The inclusive photon cross section has been measured by both CDF and UA2 and is compared to theoretical predictions.

*Presented at the Xth International Conference on Physics in Collision, Duke University, June 21-23, 1990.

1 Introduction

Since the early hadron colliders, tests of QCD have become more precise and now cover a wide range in jet energies. Figure 1 shows the inclusive jet cross section from AFS at $\sqrt{s} = 63$ GeV in the early 1980's, compared to the UA1 and UA2 results at $\sqrt{s} = 630$ GeV from the 1984-1985 runs and compared to the CDF data at $\sqrt{s} = 1800$ GeV from the 1988-1989 run. Clearly, CDF is now in a position to dominate the high energy tests of QCD and is probing the hardest collisions available. In addition to experimental progress, recent developments in theory have produced full Next-to-Leading Order QCD predictions for the inclusive jet cross section[1].

Although, quark substructure is not a part of current QCD theory, the presence of this type of new phenomena can be tested by looking for deviations from standard QCD predictions. The CDF data, at the highest center-of-mass energy, would be most sensitive to such new phenomena. Through analysis of the inclusive jet cross section, the dijet mass spectrum and the dijet angular distribution, limits can be set on the presence of quark compositeness.

Higher order processes, such as the number of multi-jet events, could also indicate the presence of new phenomena. CDF has performed a study of 3-jet events and UA2 has studied 4-, 5- and 6-jet events. In particular, UA2 has investigated the possibility of double parton scattering which would be manifested in the 4-jet sample.

Both CDF and UA2 have measured the inclusive photon cross section. In principal, the photons provide a direct probe of the gluon structure functions and are free from the effects of fragmentation. Comparison to leading order and also Next-to-Leading Order calculations will be shown.

2 Jet Identification at CDF and UA2

Both CDF and UA2 have hadronic and electromagnetic calorimeters which are segmented into cells, or towers. The natural variables for tower segmentation in collider detectors are ϕ, the azimuthal angle around the beam, and pseudo-rapidity, designated η, where $\eta = -ln(tan\theta/2)$, and θ is the polar angle with respect to the beam. The an-

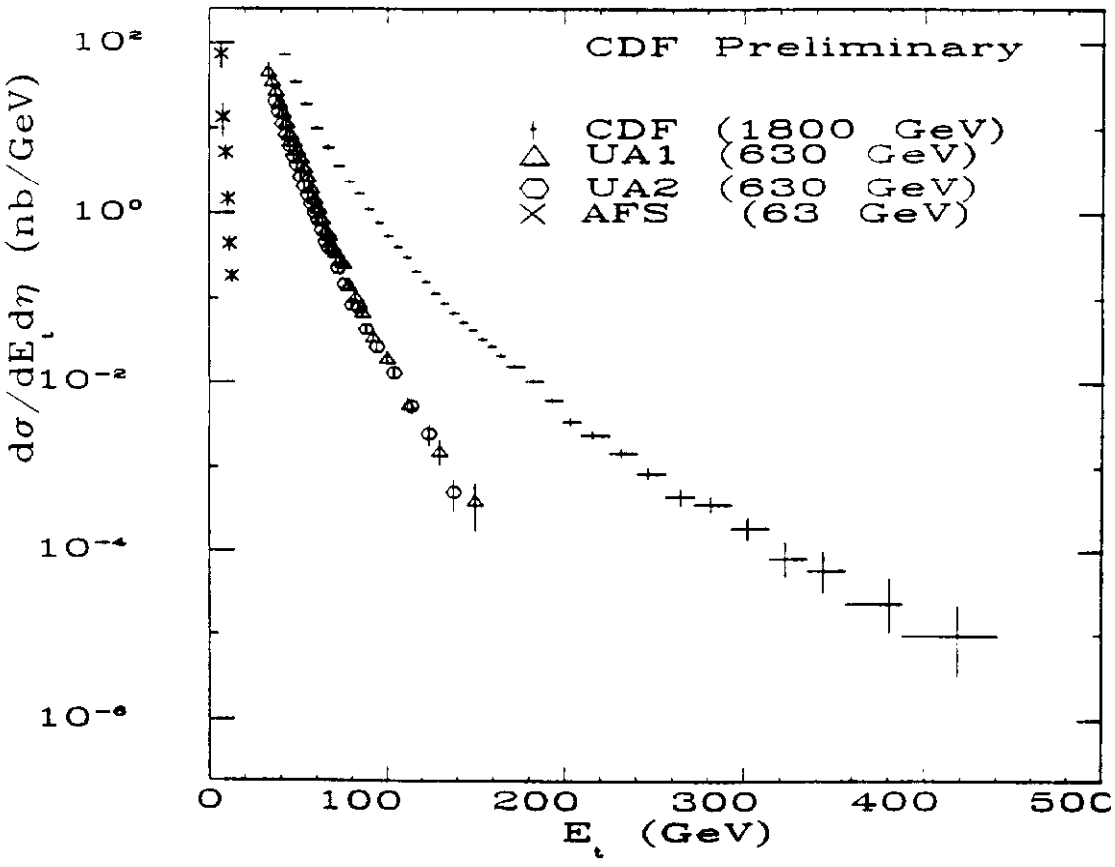

Figure 1: Inclusive Jet cross section from AFS, UA1, UA2 and CDF.

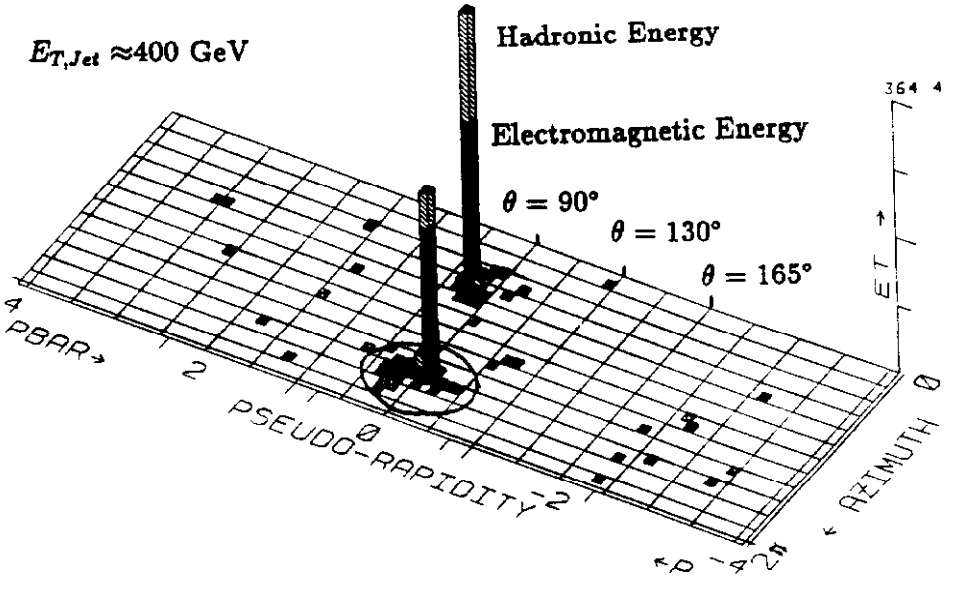

Figure 2: A CDF Jet event. The axes of the grid represent the azimuthal angle around the beamline, ϕ, and the pseudo-rapidity, defined as $-ln(tan(\theta/2))$, where θ is the polar angle with respect to the beamline. The height of each cell is proportional to its E_T .

gular coverage of the towers (0.1-0.2 in η, by 0.26-0.1 in ϕ) is smaller than the typical size of a jet. Figure 2 shows a jet event in the CDF calorimeter. This is the highest transverse energy jet in the CDF data having $E_T > 400$ GeV. A variety of algorithms have been developed for combining towers to form clusters for jet identification.

CDF uses a cone algorithm for jet identification, where the radius of the cone is defined as R=$\sqrt{\Delta\eta^2 + \Delta\phi^2}$. In Fig. 2 the circle around the energy deposition indicates roughly the boundary of the cluster cone. The jet E_T is defined by the energy of the towers in the cone and angle of the cluster centroid:

$$E_J = \sum_{i=1}^{N} E_i \ , \ \vec{P_{J,i}} = \sum_{i=1}^{N} \vec{P_i}$$

such that

$$E_{T,J} = E_J sin\theta_j \ , \text{and } sin\theta_J = P_{T,J}/P_J.$$

The sums run over the towers in the cone which have E_T >100 MeV. A cone size of R=0.7 is used in all CDF jet analyses unless otherwise indicated.

The UA2 algorithm operates with a different technique[2]. Adjacent towers with $E_T > 400$ MeV are combined. Once the towers have been grouped into clusters, the cluster E_T is defined as the scalar sum of the E_T of the individual towers:

$$E_{T,J} = \sum_{i=1}^{N} E_i sin\theta_i.$$

The results of this clustering are used in the UA2 multi-jet analyses. For the measurement of the inclusive E_T spectrum, clusters with centroids within $R < 1.3$ were merged.

3 Inclusive Jet Cross Section

For many years, Leading Order (LO) predictions for the inclusive jet cross section have existed (see, for example, [3]). In these calculations there was a large uncertainty in the normalization of the theory to the data due to the uncertainty in the choice of renormalization scale. Recently, Next-to-Leading Order (NLO) calculations have been performed[1]. In this calculation, the 3-jet matrix elements are incorporated into the calculation of the inclusive cross section through the use of a parton merging algorithm.

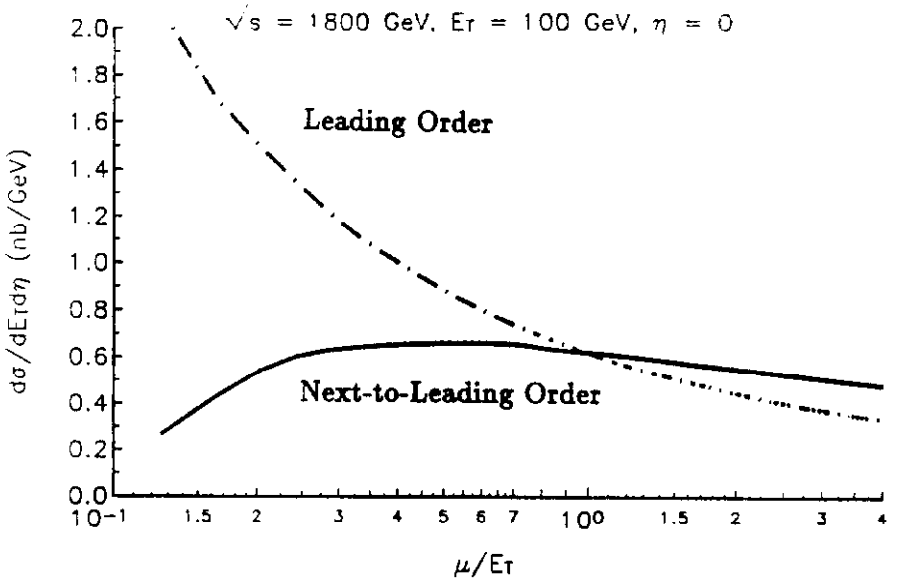

Figure 3: Predicted cross section for 100 GeV jets as a function of renormalization scale for leading order and Next-to-Leading Order QCD.

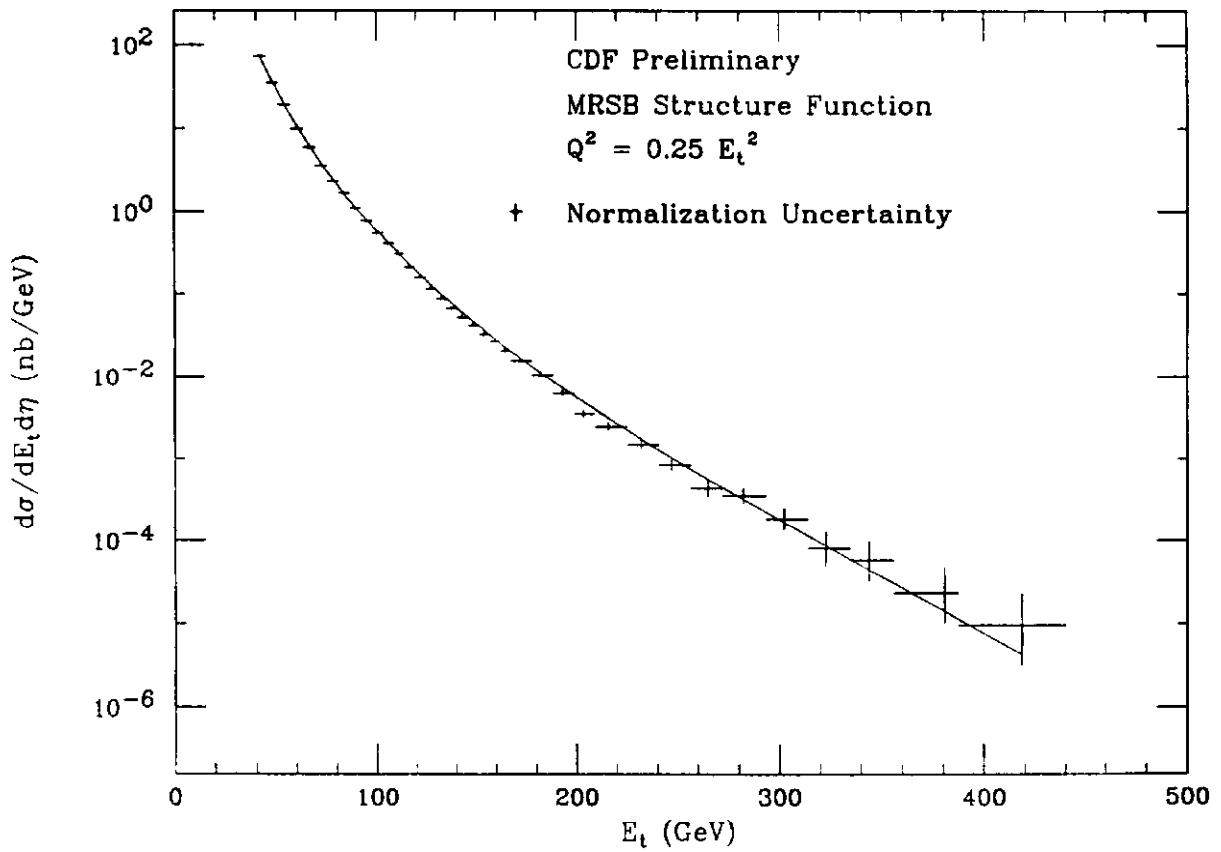

Figure 4: Inclusive jet cross section from CDF compared to the Next-to-Leading Order calculation. The theoretical prediction is absolutely normalized. Only statistical errors are shown for the data.

This algorithm is similar to the CDF cluster algorithm. A cone is defined around each parton with a radius of R=$\sqrt{\Delta\eta^2 + \Delta\phi^2}$. If two partons fall within a cone, then the E_T of the "jet" is defined as the sum E_T of the partons.

By including the Next-to-Leading term in calculation, the dependence of the cross section on the choice of renormalization scale is greatly reduced. Figure 3 shows the cross section for 100 GeV E_T jets as a function of the renormalization scale. The top curve is the result of a leading order calculation and shows a large variation, about 30%, as the scale is varied over the range of $E_T/2$ to E_T. The curve for the full NLO calculation shows a much smaller variation, about 5%, over the same range. There is still roughly a 20% uncertainty in the theoretical calculations due to differences in the structure functions. This is the dominant uncertainty in the calculations[4].

Figure 4 shows the NLO calculations compared to the CDF data with absolute normalization. The agreement is remarkable over the full range of jet E_T. Figure 5 shows the UA2 data compared to LO and NLO QCD calculations. Both theory curves are absolutely normalized. The renormalization scale of $E_T/2$ was used. In this analysis, the data has been divided into different rapidity regions. The agreement seems to be better in the central region, although the statistics are low in the high rapidity region.

The NLO calculation predicts a dependence of the inclusive jet cross section on cone size. To test this, CDF has measured the jet E_T spectrum with three cone sizes, R= 0.4, 0.7, and 1.0. Figure 6 shows the cross section for 100 GeV jets as a function of cone size from the data and as predicted by the NLO calculations. The data shows a steeper slope than the theoretical predictions.

The inclusive jet cross section can also be used to test for quark substructure. As the underlying theory for quark substructure is unknown, we look for deviations from QCD predictions. The effect of composite quarks is approximated by assuming a four-Fermion interaction with a scale Λ^*[5]. The effect of this contact term is expected to produce an increase in the number of jets above a given E_T. Figure 7 shows the CDF data compared to LO QCD and to a model that includes a contact interaction with a scale of $\Lambda^* = 950$ GeV. The theory curves are normalized to the data in a region where quark compositeness would produce little or no deviation from QCD; for this analysis, the normalization region was 80 to 160 GeV.

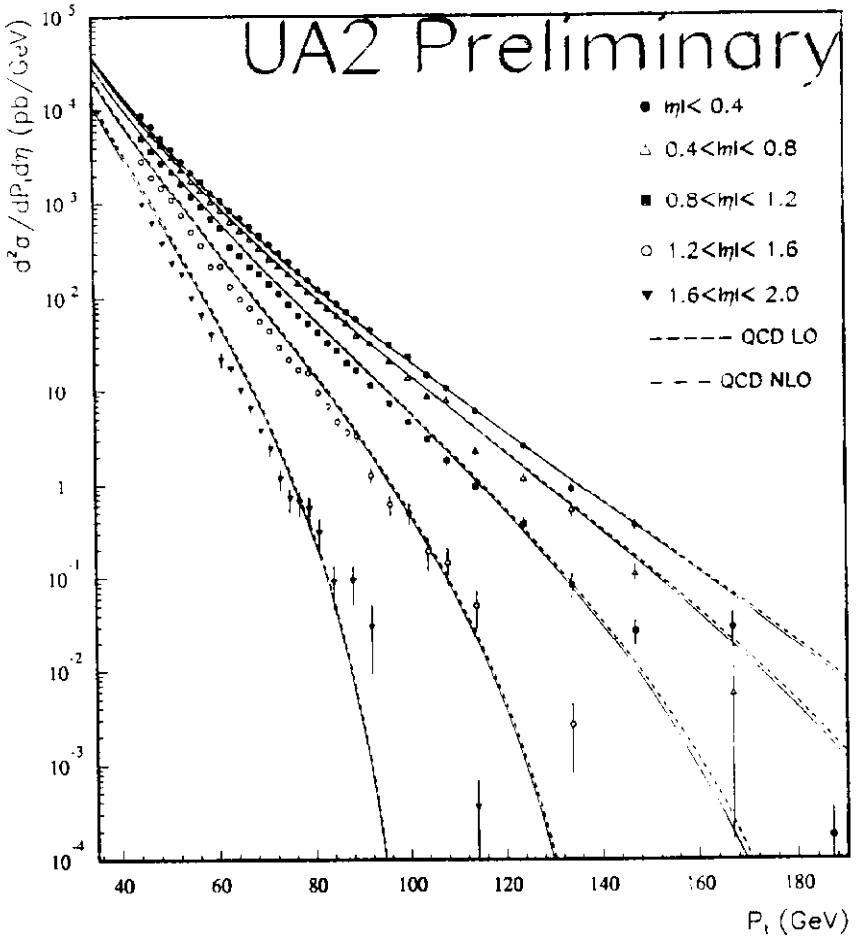

Figure 5: Inclusive Jet cross section from UA2 for different pseudorapidity regions. Leading order and Next-to-Leading Order predictions are shown. Renormalization scale was $E_T/2$ for both calculations, and they are absolutely normalized.

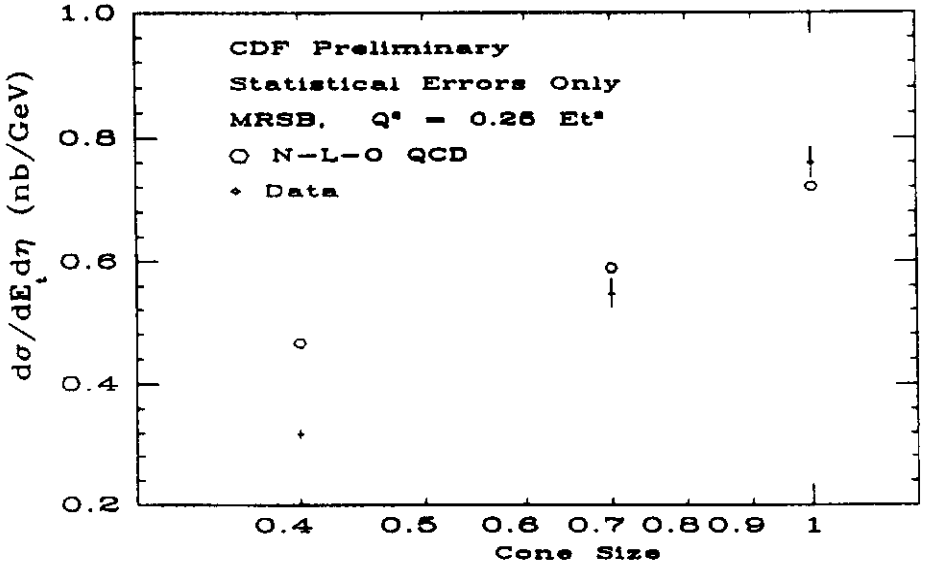

Figure 6: Dependence on cone size of the cross section for 100 GeV jets for the CDF data compared to the Next-to-Leading Order prediction.

The data is consistent with the previous limit of 950 GeV[6]. The significance of the excess of events at high E_T over the QCD predictions is under study. With statistical errors only, it is roughly 2σ over QCD, but systematic errors and correlations in the systematic errors have not yet been taken into account[6].

4 Dijet studies

Additional tests of QCD involve the study of dijet events. The cross section for dijets can be written in terms of the orthogonal variables, η_{boost}, M_{jj}, and cos θ^* where

$$\eta_{boost} = (\eta_1 + \eta_2)/2,$$

$$M_{jj} = ((E_1 + E_2)^2 - (P_1 + P_2)^2)^{1/2},$$

$$cos\theta^* = P_z/(P_x^2 + P_y^2 + P_z^2)^{1/2}.$$

If quarks were composite, they would produce an excess of events at high mass. The angular distribution for the contact interaction is isotropic and thus, the largest deviation from QCD is expected in the central region, $\theta \approx 90°$, where QCD is smallest.

Figure 8 shows the dijet mass spectrum compared to a variety of theoretical predictions. The band represents the range in the predictions for different renormalization scales and structure functions.

For the structure functions which gave the best fit to the data, the compositeness hypothesis was tested. Figure 9 shows the data compared to the theory with different compositeness scales. The theoretical predictions were normalized to the data by fitting over the full mass spectrum. The data is consistent with the limit from the inclusive jet cross section of 950 GeV[7].

The dijet scattering angle is an orthogonal variable to the invariant mass and thus provides an independent test for compositeness. The leading two jets in an event are used to define the dijet system. In the center-of-mass frame, the two jets are back-to-back, and the scattering angle, θ^*, is defined as the angle between the jets and the incoming beam.

To see the effect of including a contact term, it is more useful to plot the data as a function of χ, where $\chi = (1 + cos\theta^*)/(1 - cos\theta^*)$. The distribution of $dN/d\chi$ would be

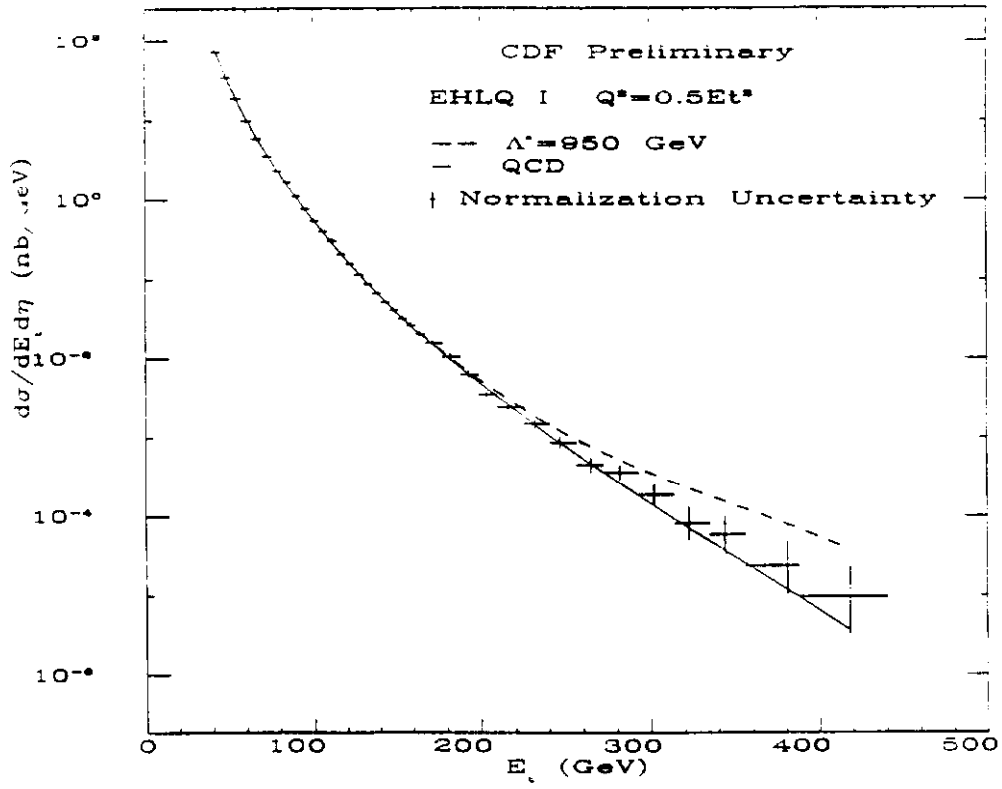

Figure 7: Inclusive Jet cross section from CDF data compared to QCD (solid) and to the model for quark substructure (dashed) with a scale Λ^*= 950 GeV. Only statistical errors are shown.

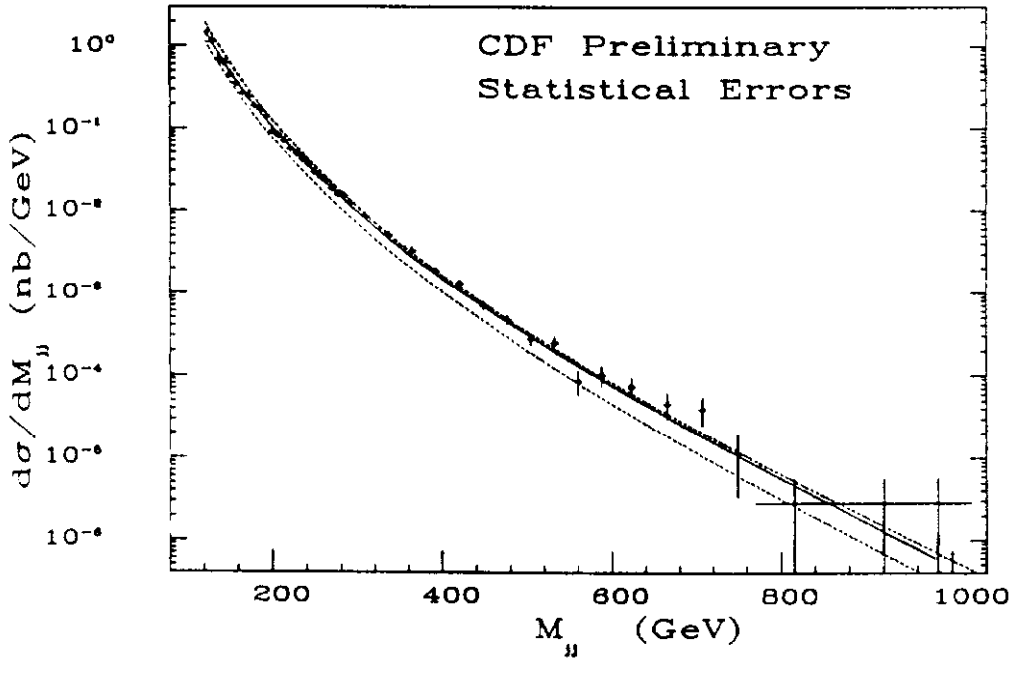

Figure 8: Dijet mass distribution from CDF.Dashed lines indicate the range of predictions for different structure functions and renormalization scales. The solid line is for DO2 structure functions with $Q^2=P_t^2$ which gave the best fit to the data.

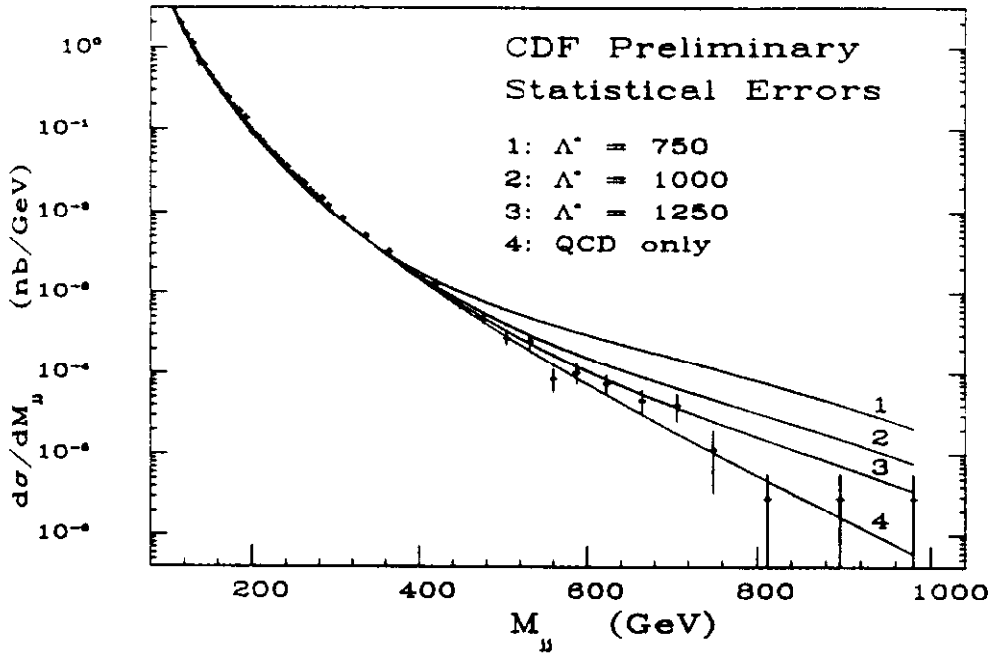

Figure 9: Dijet mass distribution from CDF. Data are compared to predictions with different compositeness scales using DO2 structure functions and $Q^2=P_t^2$.

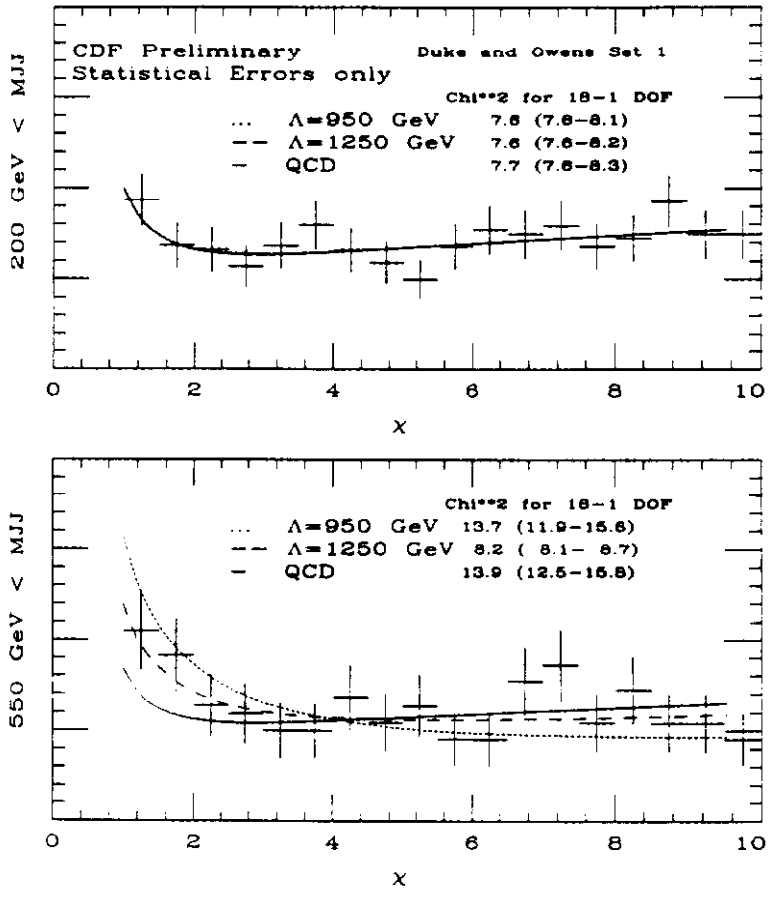

Figure 10: Dijet angular distribution from CDF. The top plot was made using a low E_T jet data sample, and the bottom plot comes from the high E_T jet data sample. At low mass there is no separation between QCD and $\Lambda^* = 950$ GeV. At high mass, there is significant separation in the theoretical predictions when a compositeness term is included.

flat for Rutherford scattering ($dN/dcos\theta^* \approx sin^{-4}\theta/2$). Figure 10 shows preliminary results for two mass bins in the CDF data. The upper plot was made using a low E_T jet event sample. The bottom plot represents the high mass region attainable with the 1988-1989 CDF data. The theoretical predictions for different compositeness scales are shown for each mass bin. In fits to the data, the normalization of the theory curve is chosen to minimize the chi-square. The range in chi-squares, shown in parentheses, represent a preliminary estimate of the uncertainty from the acceptance corrections. The data is consistent with the compositeness limit from the inclusive jet analysis.

5 Multi-jets

Events with more than two jets are expected by QCD and provide a test of the higher order calculations. The standard approach is to use a clustering algorithm and restrict both the theory and experiment to regions of phase space in which the individual jets distinguishable. For 3-jet events, the variables under study at CDF are the fractions of the maximum possible energy carried by each of the jets:

$$x_i = \frac{2E_i}{M_{3jet}},$$

where M_{3jet} is the 3-jet mass, i=3 refers to the highest energy jet and i=5 refers to the lowest energy jet in the center-of-mass frame.

Figure 11 shows a Dalitz plot and projections of energy fractions x_3 and x_4. The upper and lower corners on the right side of the Dalitz plot correspond to the infrared and collinear divergences of the 3-jet matrix elements, respectively. Cuts have been imposed to avoid these regions in both the theory and experiment. The projections are compared to the QCD predictions and to 3-body phase space. QCD is clearly preferred over phase space and shows a good fit to the data.

Another type of 3-jet study at CDF involved an event shape parameter, designated $< Q_T > /E_T$, which does not use clustering. The parameter Q_T is defined as the scalar sum of the momentum perpendicular to the transverse thrust axis, where the transverse thrust axis represents the direction of maximum energy flow in the plane transverse to the beam; $< Q_T >$ is the mean Q_T in a given slice or bin of total E_T .

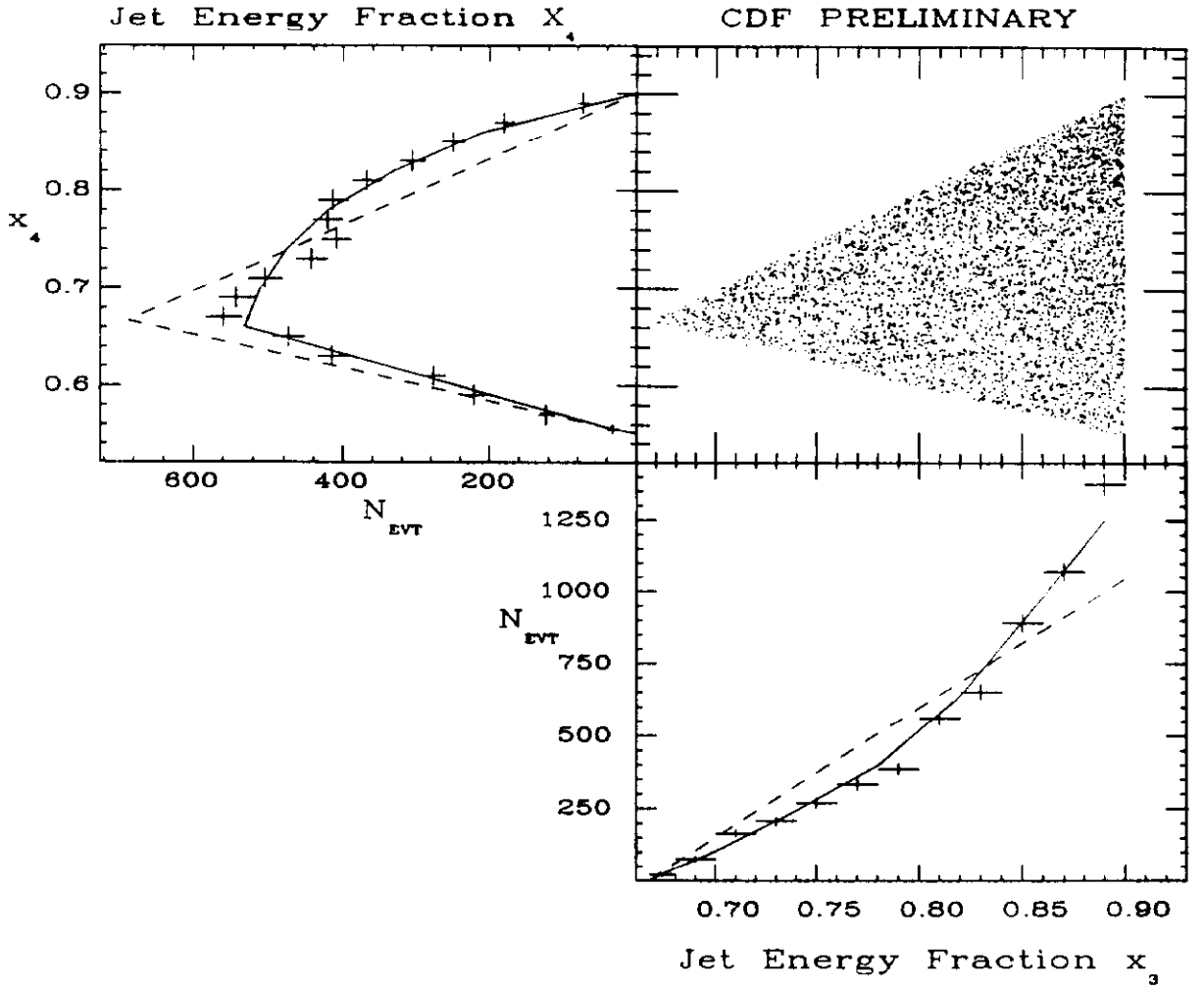

Figure 11: Dalitz plot and projections for 3-Jet energy fraction variables, x_3 and x_4. N_{EVT} represents the number of events in bins of 0.02 in x_3 or x_4. Cuts were made to avoid the QCD divergences. A Dalitz plot for phase space would be flat. The QCD (solid) and phase space (dashed) predictions for the projections are shown.

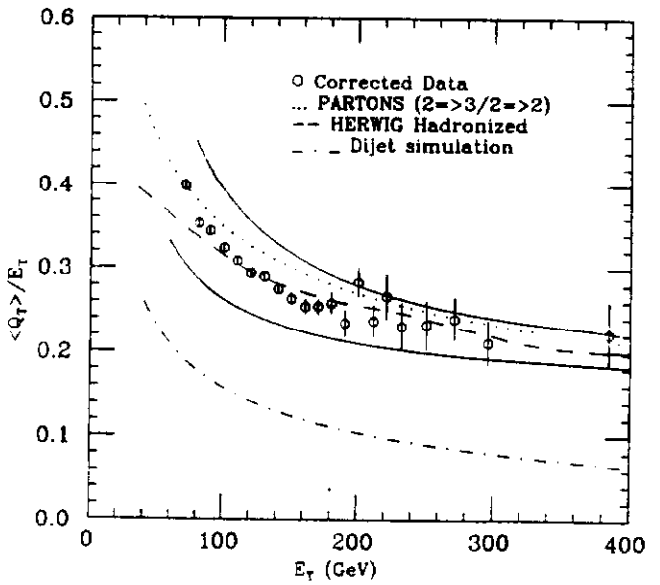

Figure 12: Global parameter $< Q_T > / E_T$ vs. E_T compared to a tree-level 3-parton calculation, the HERWIG Monte Carlo and to a tree-level 2-parton calculation plus a simple model for fragmentation.

Q_T has the property of cancelling the infra-red divergence and being stable against the collinear singularity in the 3-jet matrix elements. The theoretical evaluation of Q_T from tree-level diagrams can be performed over the full range of 3-jet configurations without imposing angular separation or energy cuts on the partons. Q_T can be evaluated from the data without the uncertainty from the choice of clustering parameters and cluster cuts. Figure 12 shows the $< Q_T > /E_T$ distribution from the data[8] compared to a parton level calculation and the full shower monte carlo HERWIG[9]. The solid lines indicate the uncertainty in the data which comes mainly from the underlying event. The dot-dashed line is the prediction from a $2 \Rightarrow 2$ parton level calculation plus a simple fragmentation model. These results indicate that either the 3-jet matrix elements, or a detailed treatment of gluon bremsstrahlung are needed to reproduce the data[8].

Events with four jets have been studied extensively by UA2[2]. Figure 13 shows the mass and sphericity distributions of the 4-jet events compared to leading order 4-jet QCD[10]. Also shown are comparisons to predictions of the angles between pairs of jets in the events. The data seems to be well modeled by the QCD predictions. In addition to 4-jet events, the cross sections for 5- and 6-jet events have been measured by UA2[2]. Figure 14 shows the measured cross section from UA2 data compared to LO QCD for 4-jets events. Also shown are the predictions for 4- and 5-jet events with the approximation that only gluons exist[11]. Note that leading order QCD reproduces the 4-jet data well, and, as expected, the gluon approximation fails to reproduce the data at high E_T.

An interesting effect that might show up in the 4-jet event sample is Double Parton Scattering (DPS). In principal, two partons in each of the colliding hadrons could undergo a hard collision. One signal for this would be an excess of 4-jet events that have two well-balanced pairs of jets. The AFS collaboration investigated this effect at much lower center-of-mass energy and attributed a significant fraction of their 4-jet events to double parton scattering[4].

In the simplest model of double parton scattering, the cross section is expected to be roughly:

$$\sigma_{DPS} = \frac{1}{2}\frac{\sigma_2^2}{\sigma_{eff}},$$

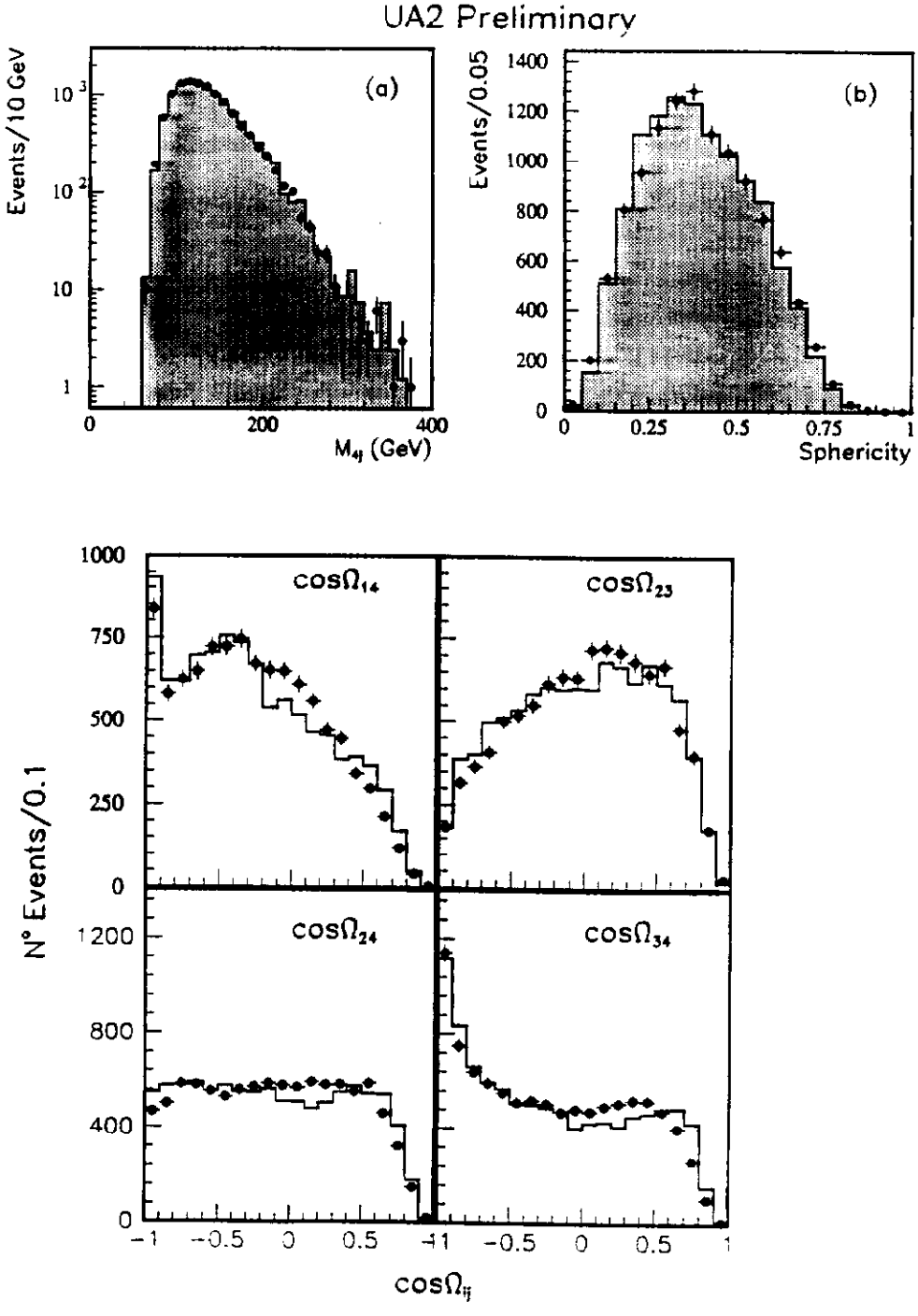

Figure 13: Mass, sphericity, and angular separation distributions for 4-jet events compared to leading order 4-jet QCD. Note that sphericity is calculated from the jets, not the individual particles. In the angular variables, 1 refers to the highest E_T jet, and Ω_{14} is the angular separation between the highest and lowest E_T jet.

where σ_2 is the 2-jet cross section, and σ_{eff} represents a new scale parameter which is of order, or less than, the total cross section of 40 mb. To simulate this process UA2 used two approaches[2]: 1) calorimeter data from two dijet events were combined into one event and then clustering was performed. This is referred to as the 2Jet-merged sample. 2) A version of PYTHIA was modified to force two hard interactions to occur in each $p\bar{p}$ collision and then clustering was performed as usual. This is referred to as the modified-PYTHIA sample and is expected to look more like QCD since effects such as radiation are taken into account.

While the agreement shown in Figure 13 of LO QCD and the 4-jet data leaves little room for double parton scattering, a limit on σ_{eff} can be derived. In addition to investigating the standard 4-jet variables such as mass, sphericity, and angular separations, UA2 found that a another variable, S, had a higher sensitivity to DPS-like events. S is defined as a measure of the P_T imbalance of the dijet pairs in an event:

$$S = \frac{1}{2} min \left[\frac{|\vec{P_{T,i}} + \vec{P_{T,j}}|^2}{|\vec{P_{T,i}}| + |\vec{P_{T,j}}|} + \frac{|\vec{P_{T,k}} + \vec{P_{T,l}}|^2}{|\vec{P_{T,k}}| + |\vec{P_{T,l}}|} \right],$$

where permutations of the indices $ijkl$ run over the four jets in the event. The combination which results in the minimum S is taken as the S for the event. Figure 15 shows the distribution in S from the data compared to LO QCD, the 2Jet-merged and modified-Pythia event samples. In a detector with perfect resolution, S $\approx$ 0 for DPS events since the 2-jet pairs will balance exactly. In a real detector, S for DPS events peaks at lower S than QCD double bremsstrahlung events.

To establish a limit on σ_{eff}, fits were performed to the data as follows: for each DPS sample and the QCD sample, the shape of the S distribution was extracted. A weight was assigned to each spectrum, N_{QCD} or N_{DPS}. In the fit to the data, these weights were adjusted such that the total, $N_{QCD} + N_{DPS}$, equaled the total number of 4-jet events in the data.

Figure 15 shows the chi-square curves for the two DPS models. The chi-square which corresponds to a 95% confidence level is used to derive a limit on the number of DPS events in the data. Table 1 shows the preliminary results of the fits and the corresponding limit on the DPS cross section. In contrast to the AFS results[4], UA2 has found that the data is consistent with a very small, or zero, fraction of DPS events.

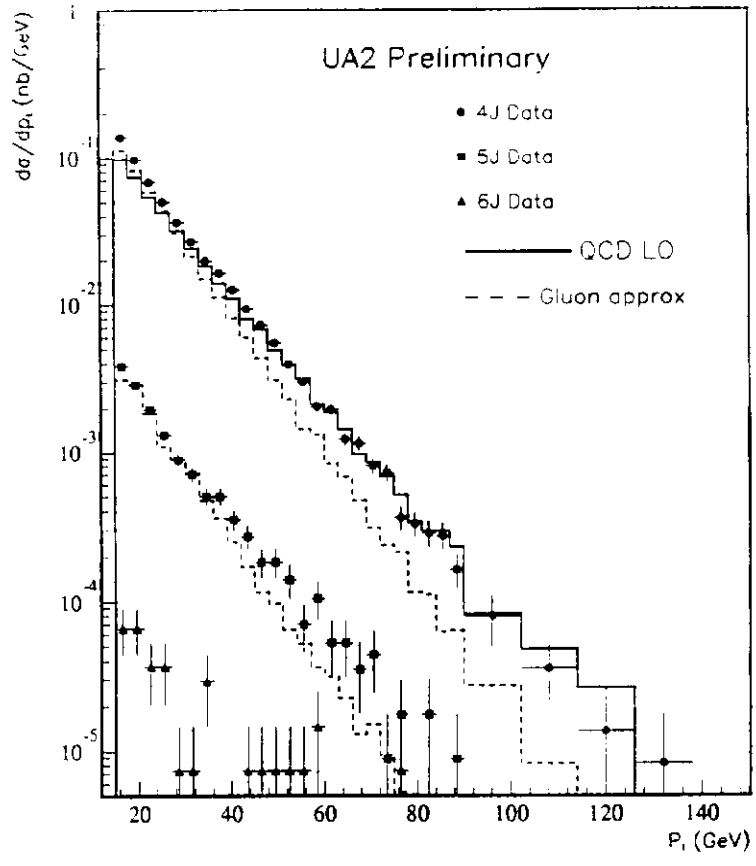

Figure 14: Measured cross section of 4-jet, 5-jet, and 6-jet events compared to leading order QCD and the gluon approximation for 4-jet and 5-jet events. The E_T of each jet in a 4-, 5- or 6-jet event is entered in the plot.

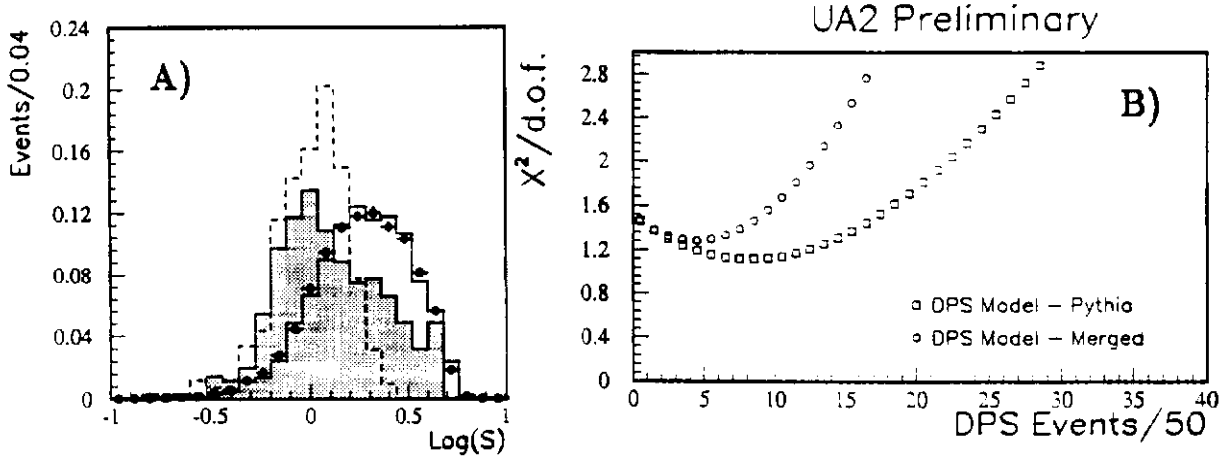

Figure 15: A) Distribution of the 4-jet variable S, for UA2 data, and leading order QCD (solid histogram). Also shown are the distributions in S for the double parton scattering models: the 2Jet-merged (dashed) and the modified-PYTHIA (shaded). B) For the variable S, the chi-square is shown as a function of number of double parton scattering events in the data.

Table 1: Preliminary UA2 DPS Fit Results

DPS Model	N_{DPS}	$\sigma_{DPS}(nb)$	σ_{eff}(mb)
Modified-PYTHIA	425±180	<0.51 at 95% C.L.	>20 at 95% C.L.
2Jet-merged	216±130	<0.26 at 95% C.L.	>39 at 95% C.L.

6 Photons

Photons produced directly from the hard collision provide a probe of the gluon structure functions and an energy measurement which is free from the effects of fragmentation. Two approaches have been used for the detection of direct photons. The first method, referred to here as the profile method, was used by CDF. Shower profiles are measured in strip chambers which are embedded at shower maximum (6 radiation lengths) in the electromagnetic calorimeter. Comparison of the shower profiles from the data with shower profiles from test beam electrons, allows the separation of photons from the background, which is mainly π^os. For P_T <35 GeV, the two photons from a π^o decay will be far enough apart to produce distinct bumps in the transverse profile. At higher P_T the two photons from a π^o decay are so close together that they produce a transverse profile which cannot be distinguished from that of a single photon.

The second method, used by both CDF and UA2, involves a preconverter located in front of the electromagnetic calorimeters. A known fraction of photons and π^os will convert in the material and a statistical subtraction of the π^o background is performed. In CDF, this analysis uses the mass in the outer shell of the central tracking chamber which corresponds to roughly 18% of a radiation length.

Figure 16a shows the P_T spectrum derived from the different methods from the CDF data[12]. The theoretical predictions are all NLO calculations and the renormalization scale is P_T . The data seems to have a steeper slope at low P_T than the theoretical predictions.

In UA2, a preconverter of 1.5 radiation lengths was used. Figure 16b shows the

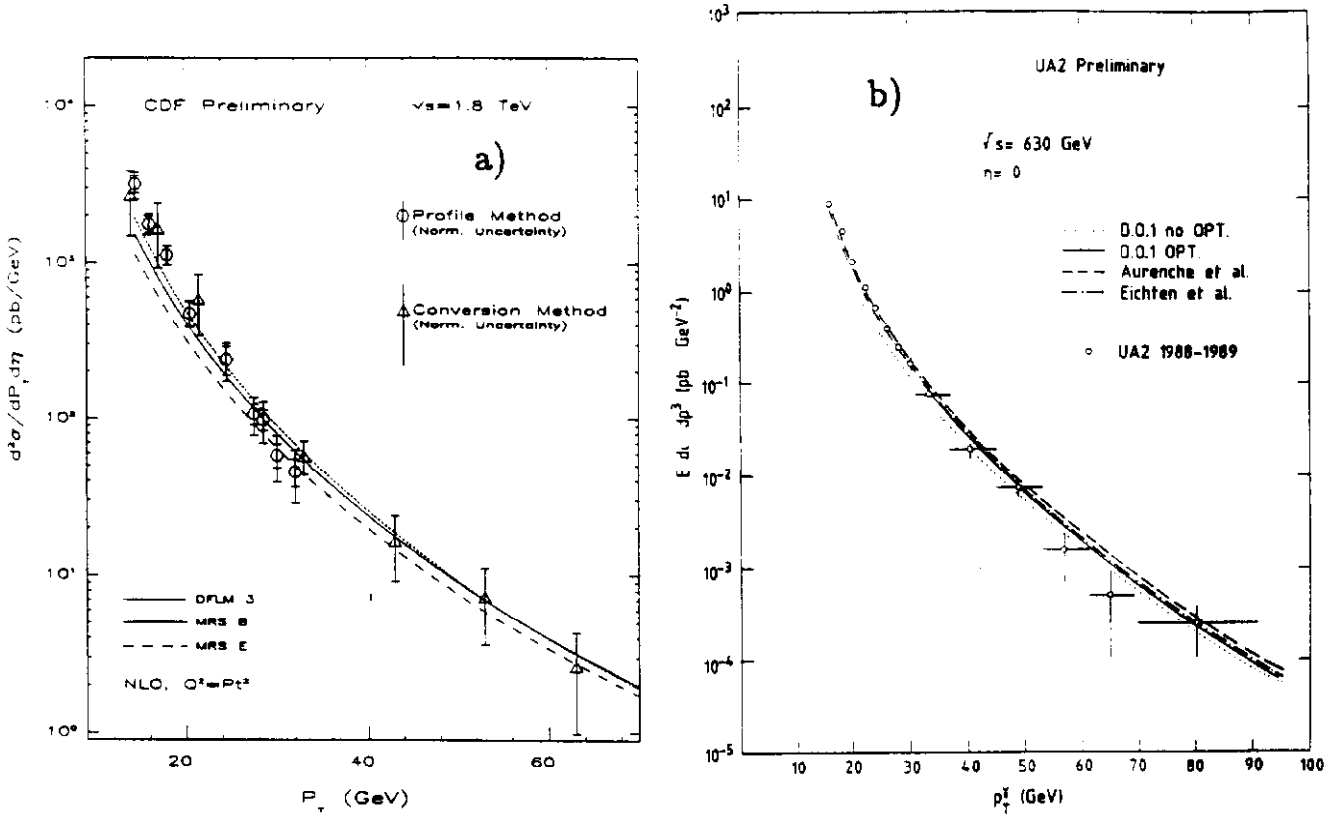

Figure 16: Inclusive photon cross sections from CDF and UA2 compared to a variety of theoretical predictions.

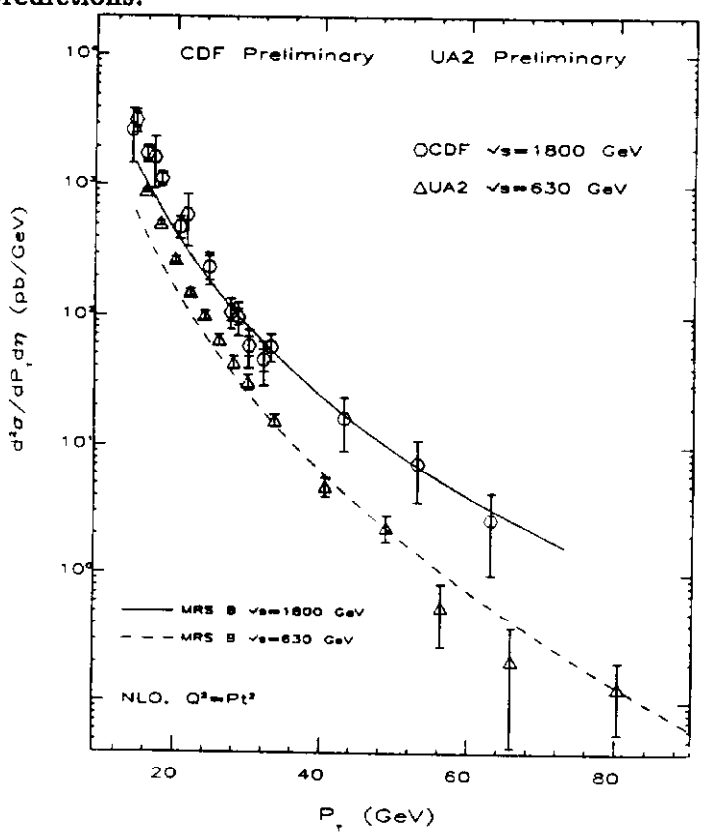

Figure 17: Inclusive photon cross section from CDF and UA2 compared to theoretical predictions using the MRSB structure functions and a renormalization scale of P_T .

P_T spectrum of the photons compared to a range of theoretical predictions. The data seems consistent with the NLO calculation, although is looks slightly higher than the curves in the low P_T region. All of the curves, except for the dotted DO1 curve, have used a renormalization scale which has been optimized to find a saddle point in the cross section[13].

Figure 17 shows both the UA2 and CDF inclusive photon spectra on the same plot compared to a NLO calculation with the same structure functions and the same choice of renormalization scale. Neither experiment is well described by the theory at low P_T . The effect of higher order terms and bremsstrahlung diagrams are under study. At present, the range in the predictions from different choices of renormalization scale and the disagreement between theory and data in the low P_T region, preclude the separation of the effects of different gluon structure functions.

7 Summary and Conclusions

The inclusive jet cross sections at UA2 and CDF are well described by LO and NLO QCD. The CDF inclusive jet cross section is consistent with the previous limit on quark substructure of 950 GeV. The dijet mass and angular distribution from the CDF data are well described by QCD and are also consistent with the compositeness limit from the inclusive jet cross section.

Kinematic variables for 3- and 4-jet events are well described by QCD. A preliminary upper limit on the double parton scattering cross section has been found from the UA2 4-jet data, and is consistent with current theoretical estimates.

The photon inclusive cross section has been measured at $\sqrt{s}$ = 630 GeV and $\sqrt{s}$ = 1800 GeV. There is some debate about the proper choice of scale and the effect of higher order terms. Most of the calculations fit the data well at high P_T .

References

[1] S. Ellis, Z. Kunszt and D. Soper, Phys. Rev. D 40 2188 (1989); U. of Oregon Preprint OITS 436 (1990),and ETH-TH/90-3.

[2] UA2 Collaboration, presented by P.Lubrano, Jet Physics with the UA2 Detector, to appear in the 'Proceedings of the 4th Recontres de Physique de la Vallee D'Aoste',La Thuile, Italy, March 1990.

[3] E. Eichten, I. Hinchliffe, K. Lane and C. Quigg, Rev. Mod. Phys. 56, 4, Oct. 1984.

[4] T. Åkesson et al., Axial Field Spectrometer Collaboration, Z.Phys. C 34,163-174 (1987).

[5] E.Eichten, K. Lane and M. Peskin, Phys. Rev. Lett. 50,811-814(1983).

[6] CDF Collaboration, presented by T. Hessing, Inclusive Jet Cross Section at $\sqrt{s} =$ 1.8TeV, to appear in the 'Proceedings of the XXVth Rencontres de Moriond', Les Arcs, Savoie, France, March 1990.

[7] CDF Collaboration, presented by P. Giannetti,The Dijet Invariant Mass at the Tevatron Collider, to appear in the 'Proceedings of the XXVth Rencontres de Moriond', Les Arcs, Savoie, France, March 1990.

[8] B.L.Flaugher, Measurement of QCD Jet Broadening in $p\bar{p}$ Collisions at 1.8 TeV, Ph.D. Thesis, Rutgers University, Oct. 1989, unpublished.

[9] G. Marchesini and B.R. Webber, Cavendish-HEP-87/8, UPRF-87-212, Dec. (1987).

[10] Z. Kunszt, W.J. Stirling, Phys. Lett. 171B, 307 (1986).

[11] Z. Kunszt, W.J. Stirling, DTP/87-6.
S.J. Parke, T.R. Taylor, Phys. Rev. Lett. 56,2459(1986).

[12] CDF Collaboration, presented by R.M.Harris, Recent Results on Direct Photons from CDF, to appear in 'Proceedings of the Workshop on Hadron Structure Functions and Parton Distributions',Fermilab,April 1990;Fermilab-Conf-90/118-E.

[13] P. Aurenche, R. Baier, M. Fontannaz, and D. Schiff, Nucl. Phys. B297(1988)661.